

Relevance of the parallel nonlinearity in gyrokinetic simulations of tokamak plasmas

J. Candy and R. E. Waltz
General Atomics, San Diego, California 92121

S. E. Parker and Y. Chen
Center for Integrated Plasma Studies, University of Colorado at Boulder, Boulder, Colorado 80309

(Received 10 May 2006; accepted 15 June 2006; published online 12 July 2006)

The influence of the parallel nonlinearity on transport in gyrokinetic simulations is assessed for values of ρ_* which are typical of current experiments. Here, $\rho_* = \rho_s/a$ is the ratio of gyroradius, ρ_s , to plasma minor radius, a . The conclusion, derived from simulations with both GYRO [J. Candy and R. E. Waltz, *J. Comput. Phys.*, **186**, 585 (2003)] and GEM [Y. Chen and S. E. Parker *J. Comput. Phys.*, **189**, 463 (2003)] is that no measurable effect of the parallel nonlinearity is apparent for $\rho_* < 0.012$. This result is consistent with scaling arguments, which suggest that the parallel nonlinearity should be $\mathcal{O}(\rho_*)$ smaller than the $\mathbf{E} \times \mathbf{B}$ nonlinearity. Indeed, for the plasma parameters under consideration, the magnitude of the parallel nonlinearity is a factor of $8\rho_*$ smaller (for $0.00075 < \rho_* < 0.012$) than the other retained terms in the nonlinear gyrokinetic equation.

© 2006 American Institute of Physics. [DOI: 10.1063/1.2220536]

It is normally assumed in both flux-tube¹⁻⁶ and global^{7,8} gyrokinetic simulations that the effect of the so-called parallel nonlinearity⁹ is negligible for modern tokamak plasmas (such as DIII-D, Ref. 10, and the Joint European Torus¹¹). The gyrokinetic ordering¹² shows that the parallel nonlinearity is a factor of $\rho_* = \rho_s/a$ smaller than the dominant linear and nonlinear terms in the gyrokinetic equations.¹²⁻¹⁴ Here, $\rho_s \doteq c_s/\Omega_{ci}$ is the ion-sound gyroradius, $\Omega_{ci} = eB/m_i$ is the ion gyrofrequency, m_i is the ion mass, and $c_s \doteq \sqrt{T_e/m_i}$ is the ion sound speed. However, some authors^{15,16} note the utility of retaining the parallel nonlinearity in particle-in-cell (PIC) simulations so that a formal energy conservation law¹⁷⁻²⁰ can be derived and monitored. It is claimed that this is a useful means by which to estimate the error generated by discrete particle noise.²¹

Going beyond simple error estimation, the authors of Ref. 22 made a systematic attempt to measure the effect of the parallel nonlinearity at different values of ρ_* . This study, based upon global simulations with the UCAN code,²³ found that at very large relative gyroradius ($\rho_* = 1/90$) the parallel nonlinearity leads to a distinct reduction in the simulated field energy. In contrast, at double the system size ($\rho_* = 1/180$) the reduction was found to be “much diminished.” The observation of some effect at $\rho_* = 1/90$ is ostensibly in agreement with other global simulations.⁹ Curiously, none of the studies that we are aware of shows results for the ion energy flux, which ought to be the quantity of greatest concern. Global PIC simulations which do show results for the ion energy flux have been carried out at $\rho_* = 1/125$ by Lee^{24,25} for parameters representative of the Cyclone base case.²⁶ In this work, which motivated the present paper, the parallel nonlinearity was found to enhance the zonal flow level and reduce the energy flux.

In this paper we report the results of both Eulerian (continuum) and particle-in-cell (PIC) simulations which measure the effect of the parallel nonlinearity over a wide range

of ρ_* . A feature of such studies which must be borne in mind is that, at some sufficiently small value of ρ_* , the results with and without the parallel nonlinearity ought to be identical. This requirement is a consequence of the gyrokinetic ordering [see, for example, Eq. (2) of Ref. 9]. Thus, if the effect of the parallel nonlinearity does not vanish as $\rho_* \rightarrow 0$, one must conclude that either the simulations are fundamentally flawed, or that the gyrokinetic ordering itself has been violated. Because typical simulations (without the parallel nonlinearity) achieve a clean, robust steady state with no violation of the gyrokinetic ordering, obtaining such a uniform limiting behavior ought to be carried out by researchers to check validity of simulations which include the parallel nonlinearity. In what follows we will define precisely what we mean by the term *parallel nonlinearity*, and give some consideration to its intrinsic conservation properties. These considerations turn out to be necessary to obtain a stable discretization scheme for inclusion of the new nonlinearity into GYRO. The literature reporting results with the parallel nonlinearity^{9,22,24} has been limited to simulations with a simplified (adiabatic) electron response. For this reason, we similarly limit our discussion and thus do not discuss the effect of the parallel nonlinearity on electrons.

In order to precisely define our terminology, we make a brief digression and write the gyrokinetic equation in conservative form using $(\mathbf{R}, v_{\parallel}, \mu)$ coordinates following Beer²⁷

$$\frac{\partial(BF)}{\partial t} + \nabla \cdot (BF\dot{\mathbf{R}}) + \frac{\partial}{\partial v_{\parallel}}(BF\dot{v}_{\parallel}) = 0. \quad (1)$$

Here, $\mu = v_{\perp}^2/(2B)$ is the magnetic moment. In the low- β limit we can make use of the identity

$$\nabla \times \mathbf{B} = B \nabla \times \mathbf{b} + \nabla B \times \mathbf{b} = 0 \quad (2)$$

to express the guiding-center velocity and acceleration in the form

$$\dot{\mathbf{R}} \doteq v_{\parallel} \mathbf{b} + \mathbf{v}_d + \mathbf{v}_E, \quad (3)$$

$$\dot{v}_{\parallel} \doteq -\frac{e}{m_i} \mathbf{b} \cdot \nabla \delta\phi - \mu \mathbf{b} \cdot \nabla B + v_{\parallel} \frac{\mathbf{v}_E \cdot \nabla B}{B}. \quad (4)$$

Physically, the quantities above are time derivatives along the phase flow of the system. On the right-hand side of Eqs. (3) and (4), the drift velocities are written as

$$\mathbf{v}_d \doteq \frac{v_{\parallel}^2 + \mu B}{\Omega_{ci} B} \mathbf{b} \times \nabla B \quad \text{and} \quad \mathbf{v}_E \doteq \frac{1}{B} \mathbf{b} \times \nabla \delta\phi. \quad (5)$$

It is straightforward to show that the gyrokinetic-Liouville theorem¹⁸ is satisfied,

$$\nabla \cdot (B\dot{\mathbf{R}}) + \frac{\partial}{\partial v_{\parallel}} (B\dot{v}_{\parallel}) = 0. \quad (6)$$

The connection between conservative and nonconservative forms can be seen clearly by rewriting Eq. (1) as

$$\frac{\partial F}{\partial t} + \underbrace{\dot{\mathbf{R}} \cdot \nabla F - \frac{\mathbf{v}_E \cdot \nabla B}{B} F}_{(1/B)\nabla \cdot (B\dot{\mathbf{R}}F)} + \underbrace{\dot{v}_{\parallel} \frac{\partial F}{\partial v_{\parallel}} + \frac{\mathbf{v}_E \cdot \nabla B}{B} F}_{(1/B)\partial/\partial v_{\parallel}(B\dot{v}_{\parallel}F)} = 0. \quad (7)$$

Following the notation and definitions in Ref. 20, we expand $F = F_0 + h$, where $F_0 \sim \mathcal{O}(1)$ represents the equilibrium Maxwellian distribution and $h \sim \mathcal{O}(\epsilon)$ are the turbulence-induced fluctuations. Equilibrium flows are neglected in the present work, so that $\delta\phi \sim \mathcal{O}(\epsilon)$. Given these orderings, the guiding-center velocity and parallel acceleration can be split into

$$\dot{v}_{\parallel} = \dot{v}_{\parallel}^{(0)} + \dot{v}_{\parallel}^{(1)} \quad (8)$$

$$\dot{\mathbf{R}} = \dot{\mathbf{R}}^{(0)} + \dot{\mathbf{R}}^{(1)}, \quad (9)$$

where a 0 superscript denotes an $\mathcal{O}(1)$ term, and a 1 superscript denotes a $\mathcal{O}(\epsilon)$ term. After making this expansion, we can identify the $\mathcal{O}(\epsilon^2)$ contribution to Eq. (7)

$$\underbrace{\mathbf{v}_E \cdot \nabla h - \frac{\mathbf{v}_E \cdot \nabla B}{B} h}_{(1/B)\nabla \cdot (B\mathbf{v}_E h)} + \underbrace{\dot{v}_{\parallel}^{(1)} \frac{\partial h}{\partial v_{\parallel}} + \frac{\mathbf{v}_E \cdot \nabla B}{B} h}_{(1/B)\partial/\partial v_{\parallel}(B\dot{v}_{\parallel}^{(1)}h)}. \quad (10)$$

This expression shows that the nonlinear terms in the gyrokinetic equation are naturally separable into two conservative nonlinear contributions, which we call the perpendicular nonlinearity and parallel nonlinearity (PNL), respectively,

$$\text{perpendicular nonlinearity: } \frac{1}{B} \nabla \cdot (h\mathbf{b} \times \nabla \delta\phi), \quad (11)$$

$$\text{parallel nonlinearity: } \frac{\partial}{\partial v_{\parallel}} \left[h \left(-\frac{e}{m} \mathbf{b} - v_{\parallel} \frac{\mathbf{b} \times \nabla B}{B^2} \right) \cdot \nabla \delta\phi \right]. \quad (12)$$

The form of the PNL as written above shows that it manifestly conserves density. It is *crucial* that this feature be reflected in any numerical algorithm that is used to evaluate

the nonlinearity. In GYRO, we observe a violent numerical instability if the PNL is differenced in a nonconservative manner.

A further remark about tokamak transport modeling is in order. Starting from the primitive full- F Fokker-Planck (FP) equation, one can derive a rigorous energy density (W) continuity equation,^{28,29}

$$\frac{\partial W}{\partial t} + \nabla \cdot \mathbf{Q} = H + S. \quad (13)$$

Here, \mathbf{Q} is the turbulent energy flux, $H = \delta\mathbf{j} \cdot \delta\mathbf{E}$ is the turbulent heating, and S represents the atomic and other external sources. We emphasize that H arises directly from the parallel nonlinearity in the FP equation, as discussed in detail in Ref. 28. Steady-state profiles are obtained as the solution of the problem in the limit $\partial/\partial t \rightarrow 0$. Presently, gyrokinetic codes solve the relatively simple reduced problem of computing h given fixed F_0 , rather than the self-consistent problem of finding $F = F_0 + h$ given S . To solve Eq. (13) when computing h given F_0 , one would first evaluate the terms $\mathbf{Q}(h)$ and $H(h)$, update F_0 , and repeat to convergence. A remarkable finding of Ref. 28 is that, on transport space- and time scales, H and S enter at the same order in ρ_* in Eq. (13), thus making it important to retain the PNL (via H) in the transport equation. However, on turbulence space- and time scales, the PNL enters \mathbf{Q} at lower order in ρ_* than the dominant terms. This reasoning leads us to the tentative conclusion that the natural place to include the PNL is in the transport equation (as an effective source) and not in the gyrokinetic equation for h . Thus, the present paper is simply a numerical verification of this ordering argument.

The GYRO³⁰ simulations presented herein use the *GA standard case* parameters.³¹ These are $a/L_{Ti} = 3.0$, $a/L_{ni} = 1.0$, $R/a = 3.0$, $r/a = 0.5$, $s = 1$, $q = 2$, and $T_e = T_i$. Simple unshifted circular geometry and *nonperiodic boundary conditions* are used. Here, a and R are the plasma minor and major radii, respectively. To ensure smoothness in velocity-space, GYRO simulations also include a small amount of ion-ion collisions (pitch-angle scattering): $(a/c_s)v_{ii} = 0.01$. The perpendicular box size is $(L_x, L_y)/\rho_s = (130, 130)$, such that $x \rightarrow r$ is the radial coordinate and is the second coordinate perpendicular to \mathbf{B} . We have defined the box size in units of the ion sound gyroradius, $\rho_s \doteq c_s/\Omega_{ci}$, with $c_s \doteq \sqrt{T_e/m_i}$ the ion sound speed. We use $n_x = 128$ radial gridpoints, so that $\Delta x = \rho_s$, and $n_{\theta} = 16$ complex toroidal modes such that $0 \leq k_{\theta} \rho_s \leq 0.72$. The parallel resolution is set to $n_{\theta} = 10$ points per passing orbit (i.e., per sign of velocity). Finally, we use a 128-point velocity-space grid (8 energies, 8 pitch angles, and 2 signs of velocity). The maximum simulated energy is $\epsilon \leq 6T_i/m_i$. This velocity-space resolution is typical of GYRO production runs.^{1,32,33} Furthermore, the GYRO velocity grids are highly structured, so as to provide maximal accuracy in the calculation of integrals of the distribution function.³⁰ The GEM (Ref. 6) simulations, on the other hand, use the *Cyclone base case* parameters.^{26,34} These are $a/L_{Ti} = 2.5$, $a/L_{ni} = 0.8$, $R/a = 2.8$, $r/a = 0.5$, $s = 0.8$, $q = 1.4$, and $T_e = T_i$. Simple unshifted circular geometry and periodic boundary conditions are used. The perpendicular

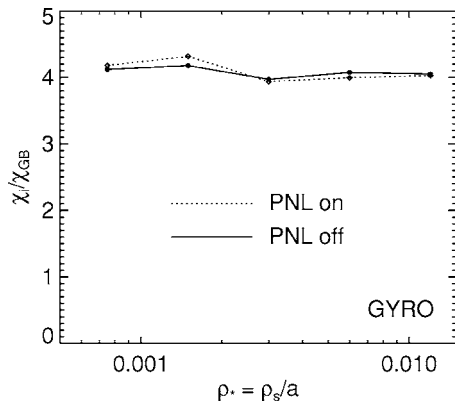


FIG. 1. GYRO ρ_* scan comparing simulations with parallel nonlinearity on (dotted line) to off (solid line). No significant effect is observed over the entire simulated range.

box size was $(L_x, L_y)/\rho_s = (256, 256)$ at a velocity-space resolution of 32 particles-per-cell (PPC). Thus, the area of the perpendicular box is four times larger than in GYRO, while the number of velocity-space points per real-space cell is four times smaller.

First, we performed GYRO simulations spanning a physically relevant interval in ρ_* ; namely $\rho_* = (0.00075, 0.0015, 0.003, 0.006, 0.012)$. Simulations were carried out over the time interval $0 \leq (c_s/a)t \leq 1500$ and data were averaged over $200 \leq (c_s/a)t \leq 1500$. It was decided to run very long simulations in order to minimize statistical error. Figure 1 compares simulations with the parallel nonlinearity absent (solid curve) to simulations with the parallel nonlinearity included (dotted curve). The result is that, within statistical uncertainty, the parallel nonlinearity does not have a discernible effect on the ion heat diffusivity. We remark that the solid curve is expected, *a priori*, to be independent of ρ_* since the equations contain no explicit ρ_* dependence (this is a well-known feature of the local limit). Thus, the ρ_* variation in the solid curve is statistical in nature, and ought to vanish as the simulation time increases further.

It is illuminating to look more closely at the added term, Eq. (12), by comparing its size in an absolute norm to the size of the full right-hand side (RHS) of the gyrokinetic equation. In detail, we write the ion gyrokinetic equation schematically as

$$\frac{\partial h}{\partial t} = \text{RHS} = \text{RHS}_{\text{main}} + \text{RHS}_{\text{PNL}}, \quad (14)$$

where RHS_{main} represents the terms normally retained in the gyrokinetic ordering¹² and RHS_{PNL} is given by the negative of Eq. (12). It is well-known that RHS_{PNL} is one order in ρ_* smaller than the RHS_{main} , and this feature is clearly reflected in the results plotted in Fig. 2. A fixed scaling (with magnitude of approximately $8\rho_*$) in ρ_* is obtained over almost the entire simulated range—with only a very weak breaking of the scaling at the largest value $\rho_* = 0.012$. The (somewhat unphysical) norm is defined as a sum over all gridpoints

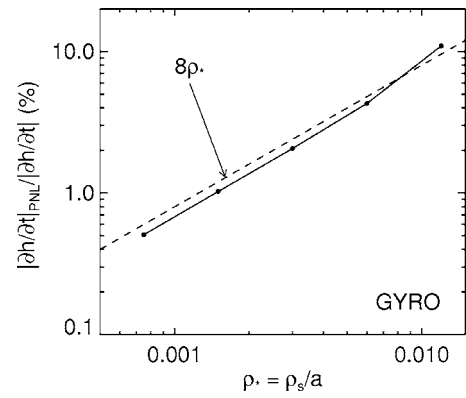


FIG. 2. Magnitude of the parallel nonlinearity compared to the entire right-hand side of the gyrokinetic equation for the scan shown in Fig. 1.

$$|\text{RHS}| \doteq \frac{1}{n_p} \sum_{p=1}^{n_p} |\text{RHS}_p| \quad \text{with } p = (\mathbf{R}, \lambda, \varepsilon). \quad (15)$$

Even though the size of the PNL in this absolute norm is 10% of the entire right-hand side, the effect on transport is insignificant. One might speculate that is perhaps related to the fact that the PNL is a density-conserving perturbation (i.e., the PNL conserves density at every point in space).

Next, independent simulations were carried out with the GEM code at a single value of $\rho_* = 0.0028$. Unlike the GYRO simulations, the GEM runs used the Cyclone base case parameters.²⁶ Since the simulations were local, the radial average of the $n=0$ component of the gyrokinetic equation,

$$\frac{1}{L} \int_0^L dr (\text{RHS}_{\text{PNL}})_{n=0}, \quad (16)$$

was subtracted from the total right-hand side to enforce radial periodicity. Simulations were run over the interval $0 \leq (c_s/a)t \leq 500$, as shown in Fig. 3. Taking time averages over the range $100 \leq (c_s/a)t \leq 500$ gives the results $\chi_i/\chi_{\text{GB}} \approx 1.7$ (PNL off, solid curve) and $\chi_i/\chi_{\text{GB}} \approx 1.8$ (PNL on, dotted curve). Like the GYRO results, the GEM simulations do not show a difference that is statistically significant; that is, the deviation between the two runs is comparable to the ex-

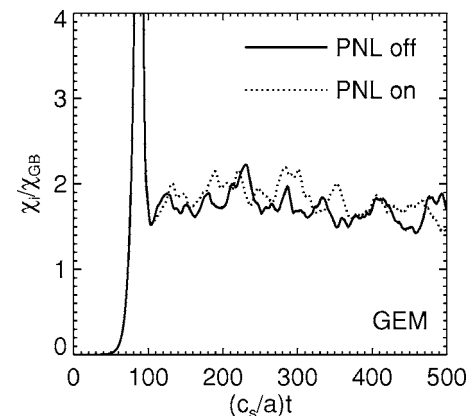


FIG. 3. GEM data comparing simulations with parallel nonlinearity off (solid line, with time-average $\chi_i/\chi_{\text{GB}} \approx 1.7$) and on (dotted line, with time-average $\chi_i/\chi_{\text{GB}} \approx 1.8$). The difference is not significant.

pected difference between two runs with identical physics and different initial conditions. Thus, we have arrived at the same conclusion using different numerical algorithms (Eulerian and PIC) with substantially different simulation resolutions. As we have emphasized earlier, the final result is unsurprising. Given that the parallel nonlinearity is small in magnitude and, with respect to a rigorous ordering, formally negligible, it would indeed be worrisome if the PNL had a significant effect in simulations.

In summary, we emphasize

- (1) The parallel nonlinearity is formally one order in ρ_* smaller than the effects normally included in gyrokinetic simulations.
- (2) Neither GYRO nor GEM measures a significant effect of the parallel nonlinearity over the range $0.0075 \leq \rho_* \leq 0.012$.
- (3) Our experience indicates that simulations which include the parallel nonlinearity must ensure that the numerical treatment is manifestly density conserving.

The authors would like to thank W. M. Nevins for his assistance, and F. L. Hinton for numerous helpful conversations.

This work was supported by U.S. Department of Energy Grant DE-FG03-95ER54309 and Cooperative Agreement No. DE-FC02-05ER54186.

¹J. Candy, Phys. Plasmas **12**, 072307 (2005).

²Y. Chen, S. E. Parker, B. I. Cohen, A. M. Dimits, W. M. Nevins, D. Schumaker, V. K. Decyk, and J. N. Leboeuf, Nucl. Fusion **43**, 1121 (2003).

³D. W. Ross and W. Dorland, Phys. Plasmas **9**, 5031 (2002).

⁴A. M. Dimits, B. I. Cohen, W. M. Nevins, and D. E. Schumaker, Nucl. Fusion **40**, 1725 (2001).

⁵F. Jenko, T. Dannert, and C. Angioni, Fusion Energy **47**, 195 (2005).

⁶Y. Chen and S. E. Parker, J. Comput. Phys. **189**, 463 (2003).

⁷J. Candy and R. E. Waltz, Phys. Rev. Lett. **91**, 045001 (2003).

⁸Z. Lin and T. S. Hahm, Phys. Plasmas **11**, 1099 (2004).

⁹L. Villard, P. Angelino, A. Bottino, S. J. Allfrey, R. Hatzky, Y. Idomura, O. Sauter, and T. M. Tran, Fusion Energy **46**, B51 (2004).

¹⁰J. L. Luxon, Nucl. Fusion **42**, 6114 (2002).

¹¹P. H. Rebut, R. J. Bickerton, and B. E. Keen, Nucl. Fusion **25**, 1011 (1985).

¹²E. A. Frieman and L. Chen, Phys. Fluids **25**, 502 (1982).

¹³T. Antonsen and B. Lane, Phys. Fluids **23**, 1205 (1980).

¹⁴M. Kotschenreuther, G. Rewoldt, and W. M. Tang, Comput. Phys. Commun. **88**, 128 (1995).

¹⁵Y. Idomura, S. Tokuda, and Y. Kishimoto, Nucl. Fusion **43**, 234 (2003).

¹⁶L. Villard, S. J. Allfrey, A. Bottino, M. Brunetti, G. L. Falchetto, V. Grandgirard, R. Hatzky, J. Nührenberg, A. G. Peeters, O. Sauter, S. Sorge, and J. Vaclavik, Nucl. Fusion **44**, 172 (2004).

¹⁷D. H. E. Dubin, J. A. Krommes, C. Oberman, and W. W. Lee, Phys. Fluids **26**, 3524 (1983).

¹⁸T. S. Hahm, Phys. Fluids **31**, 2670 (1988).

¹⁹A. Brizard, J. Plasma Phys. **41**, 541 (1989).

²⁰J. Candy and R. E. Waltz, Phys. Plasmas **13**, 032310 (2006).

²¹W. M. Nevins, G. W. Hammett, A. M. Dimits, W. Dorland, and D. E. Schumaker, Phys. Plasmas **12**, 122305 (2005).

²²J. C. Kniep, J.-N. Leboeuf, and V. K. Decyk, Comput. Phys. Commun. **164**, 98 (2004).

²³R. D. Sydora, V. K. Decyk, and J. M. Dawson, Plasma Phys. Controlled Fusion **38**, A281 (1996).

²⁴Z. Lin, G. Rewoldt, S. Ethier, T. S. Hahm, W. W. Lee, J. Lewandowski, Y. Nishimura, and W. X. Wang, J. Phys.: Conf. Ser. **16**, 16 (2005).

²⁵W. W. Lee, Bull. Am. Phys. Soc. **49**, 135 (2004).

²⁶A. M. Dimits, G. Bateman, M. A. Beer, B. I. Cohen, W. Dorland, G. W. Hammett, C. Kim, J. E. Kinsey, M. Kotschenreuther, A. H. Kritiz, L. L. Lao, J. Mandrekas, W. M. Nevins, S. E. Parker, A. J. Redd, D. E. Schumaker, R. Sydora, and J. Weiland, Phys. Plasmas **7**, 969 (2000).

²⁷M. A. Beer and G. W. Hammett, Phys. Plasmas **3**, 4046 (1996).

²⁸F. L. Hinton and R. E. Waltz, "Gyrokinetic Turbulent Heating," General Atomics Report GA-A25411, Phys. Plasmas (submitted).

²⁹G. G. Howes, S. C. Cowley, W. Dorland, G. W. Hammett, E. Quataert, and A. A. Schekochihin, "Astrophysical gyrokinetics: Basic equations and linear theory," Astrophys. J. (to be published).

³⁰J. Candy and R. E. Waltz, J. Comput. Phys. **186**, 545 (2003).

³¹R. E. Waltz, G. R. Kerbel, J. Milovich, and G. W. Hammett, Phys. Plasmas **2**, 2408 (1995).

³²C. Estrada-Mila, J. Candy, and R. E. Waltz, Phys. Plasmas **12**, 022305 (2005).

³³J. E. Kinsey, R. E. Waltz, and J. Candy, Phys. Plasmas **12**, 062302 (2005).

³⁴J. Candy, R. E. Waltz, and W. Dorland, Phys. Plasmas **11**, L25 (2004).